Appendix 1:

Using the ignition delay times, the octane number calculations can hence be made by:

$$RON = 751.8 - 452.3e^{-\frac{IDT}{0.0007514}} - 646e^{-\frac{IDT}{23.05}} \quad (1)$$

The predictions based on the equation are given in Fig. A1. Similar double exponential fits have previously been suggested for RON-IDT relationship [4, 64]. As it can be observed, the equation holds well for high-octane numbers, while qualitative agreement holds across the full range of IDT. The black dots represent the experimental data coupled with ignition delay times calculated from Chemkin [65]. The red line represents the curve fit of the points based on Eq. (1).

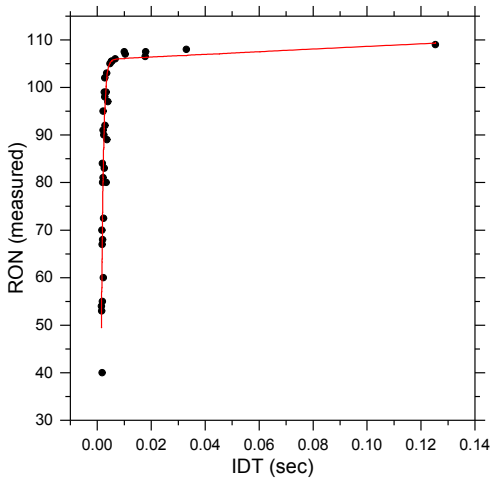

Figure A1: Experimentally obtained RON values plotted against simulated ignition delay time data at T_o 750K and P_o 40 bar, is shown in black dots. A double exponential curve fit is shown in red curve. In the inset is the comparison of predicted value of RON from the double exponential curve fit to the obtained experimental values, from literature. R^2 value for the curve fit is 0.8.

Based on the homogeneous ignition delay calculations, equation 1 was proposed to predict RON, the non-linear trend of octane increase with ethanol addition is qualitatively replicated as in the experiments, as shown in Fig. A2. There are, however, quantitative deviations in lower ethanol fractions. Such mixtures have not been considered for CSP analysis.

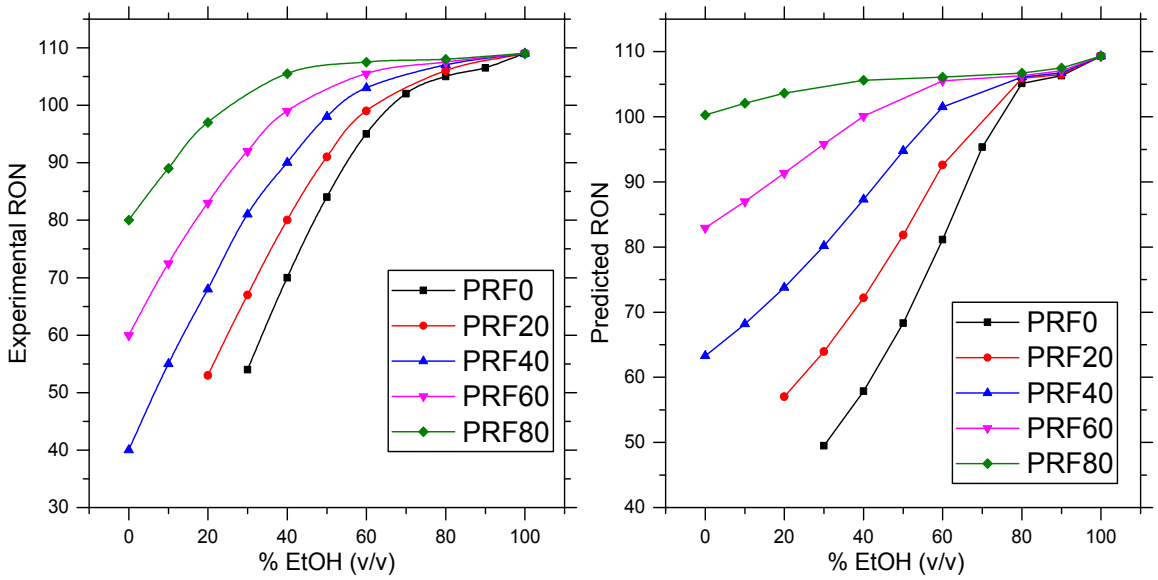

Figure A2: Measured (left) and predicted (right) octane numbers (based on equation 1) of varying ethanol blends (v/v). Experimental data from [11]. This data set is used for obtaining the RON-IDT correlation and the temperature-pressure boundary condition for subsequent batch reactor simulations. Only PRF0 is used for subsequent calculations.

Ignition delay times (in sec) calculated for each of the blends are shown in Fig. A3. Ethanol addition increases the ignition delay time exponentially.

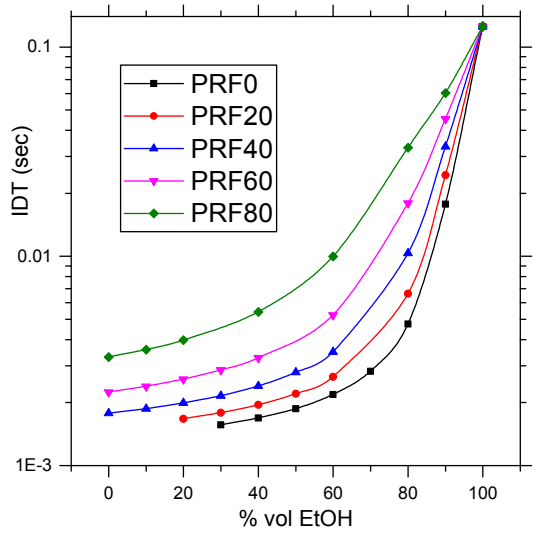

Figure A3: Ignition delay times of varying ethanol blends (v/v), calculated from homogeneous batch reactor simulations at T_o 750K and P_o 40bar.

Experimental measurements from [11] are compared in Figure A4 in terms of volume and mole fraction of ethanol in PRFs. The non-linearity in the lower vol.% is suppressed, while non-linearity is seen at higher blend % when considering same blends on mole fraction.

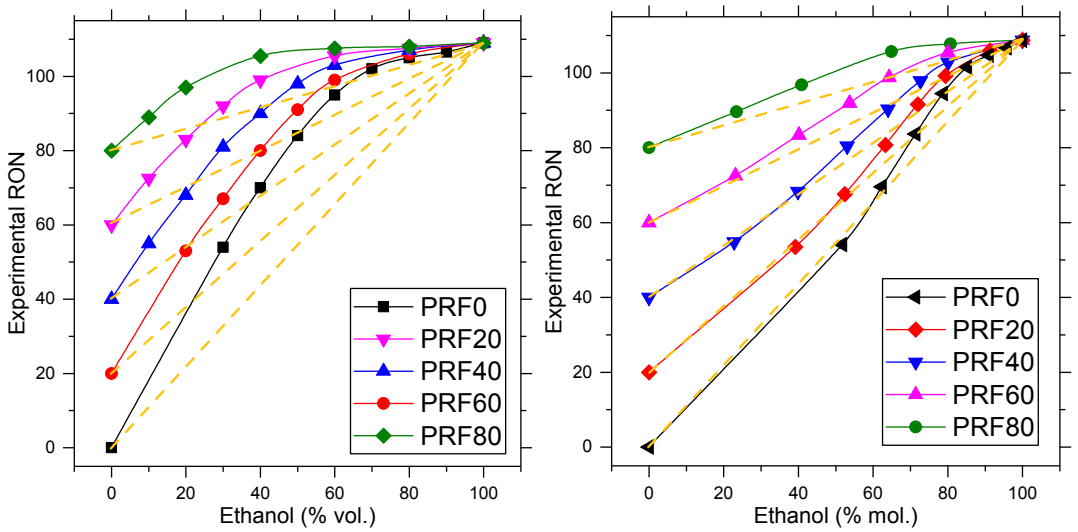

Figure A4: Measured RON by [11] displayed on volume and mole fraction. Linear-by-vol/mol. line is shown in yellow dashed lines for each PRF-ethanol mixture. Non-linearity in octane boosting tendency is suppressed and delayed (in terms of % additive) when plotted on mole fraction of ethanol in PRF.

Appendix 2:

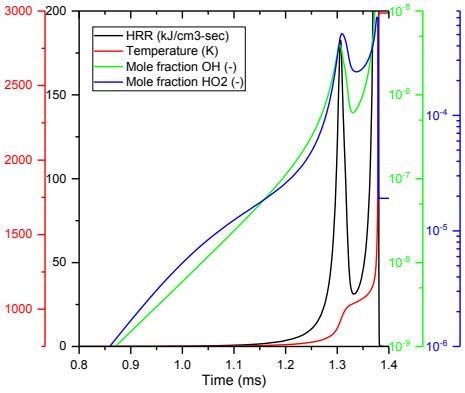

Figure B1: Reactivity evolution for pure *n*-heptane for 750K and 40 bar.

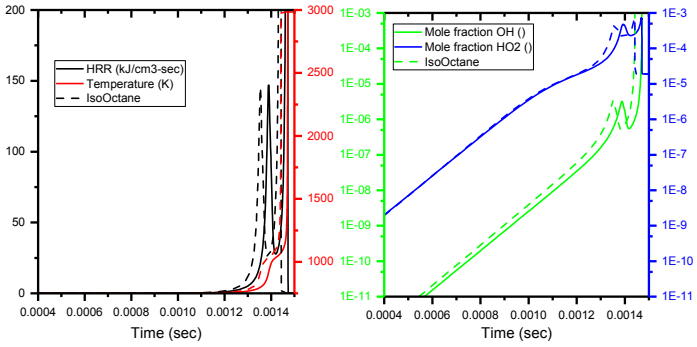

Figure B2: Reactivity evolution for mixture of 90% *n*-heptane and 10% *iso*-octane/ethanol (a) heat release rate and temperature, (b) mole fraction of OH and HO_2. The values for ethanol-*n*-heptane are given in solid lines and *iso*-octane-*n*-heptane mixture are given in dashed lines.

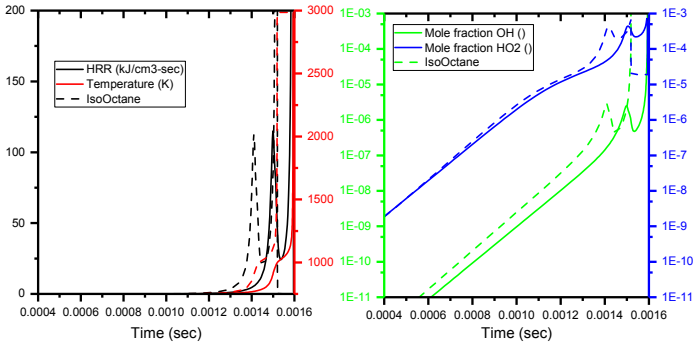

Figure B3: Reactivity evolution for mixture of 80% *n*-heptane and 20% *iso*-octane/Ethanol. (a) heat release rate and temperature, (b) mole fraction of OH and HO_2. The values for ethanol-*n*-heptane are given in solid lines and *iso*-octane-*n*-heptane mixture are given in dashed lines.

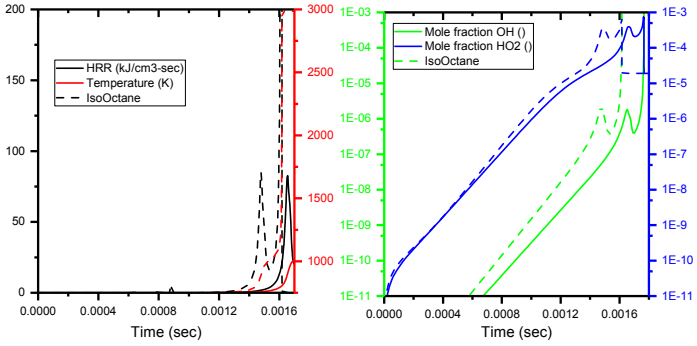

Figure B4: Reactivity evolution for mixture of 70% *n*-heptane and 30% *iso*-octane/ethanol. (a) heat release rate and temperature, (b) mole fraction of OH and HO_2. The values for ethanol-*n*-heptane are given in solid lines and *iso*-octane-*n*-heptane mixture are given in dashed lines.

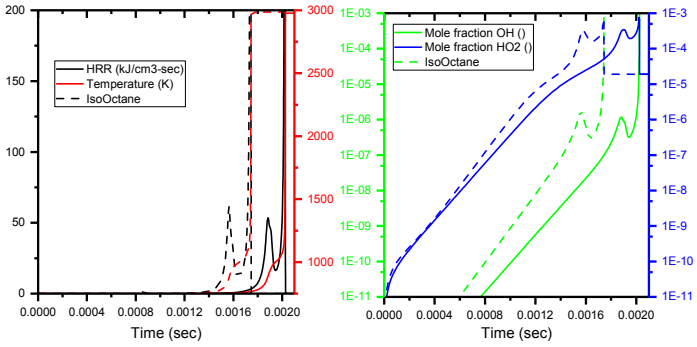

Figure B5: Reactivity evolution for mixture of 60% *n*-heptane and 40% *iso*-octane/ethanol. (a) heat release rate and temperature, (b) mole fraction of OH and HO_2. The values for ethanol-*n*-heptane are given in solid lines and *iso*-octane-*n*-heptane mixture are given in dashed lines.

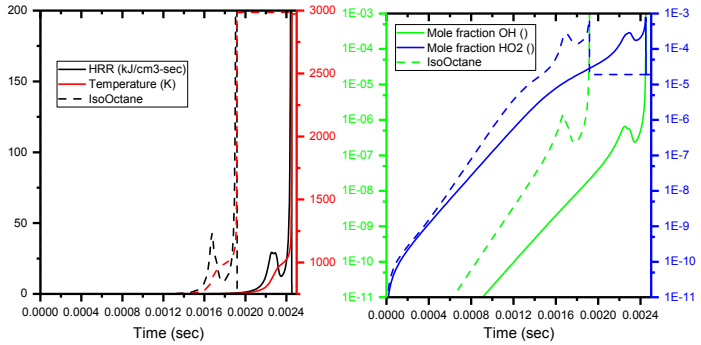

Figure B6: Reactivity evolution for mixture of 50% *n*-heptane and 50% *iso*-octane/ethanol. (a) heat release rate and temperature, (b) mole fraction of OH and HO_2. The values for ethanol-*n*-heptane are given in solid lines, and *iso*-octane-*n*-heptane mixture are given in dashed lines.

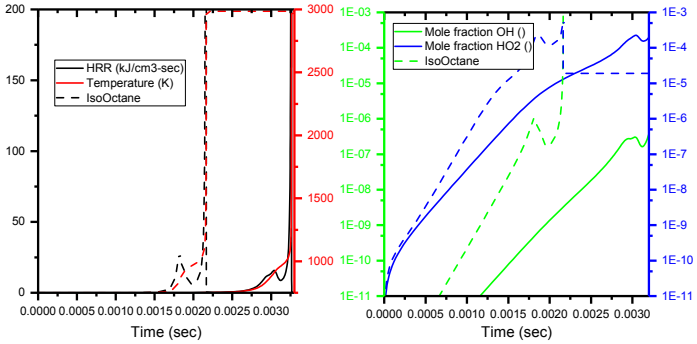

Figure B7: Reactivity evolution for mixture of 40% *n*-heptane and 60% *iso*-octane/ethanol. (a) heat release rate and temperature, (b) mole fraction of OH and HO_2. The values for ethanol-*n*-heptane are given in solid lines, and *iso*-octane-*n*-heptane mixture are given in dashed lines.

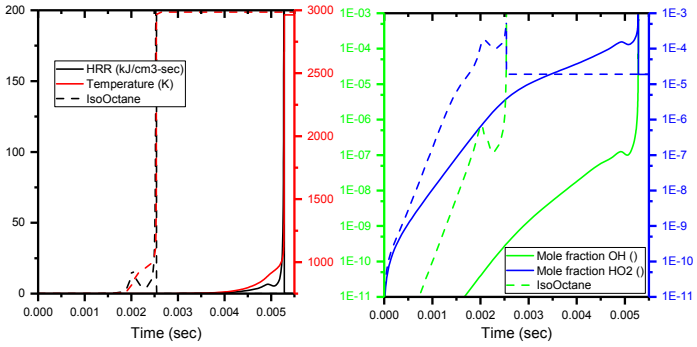

Figure B8: Reactivity evolution for mixture of 30% *n*-heptane and 70% *iso*-octane/ethanol. (a) heat release rate and temperature, (b) mole fraction of OH and HO_2. The values for ethanol-*n*-heptane are given in solid lines and *iso*-octane-*n*-heptane mixture are given in dashed lines.

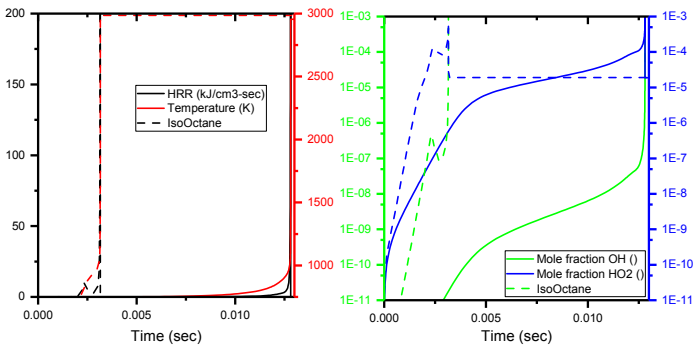

Figure B9: Reactivity evolution for mixture of 20% *n*-heptane and 80% *iso*-octane/ethanol. (a) heat release rate and temperature, (b) mole fraction of OH and HO_2. The values for ethanol-*n*-heptane are given in solid lines and *iso*-octane-*n*-heptane mixture are given in dashed lines.

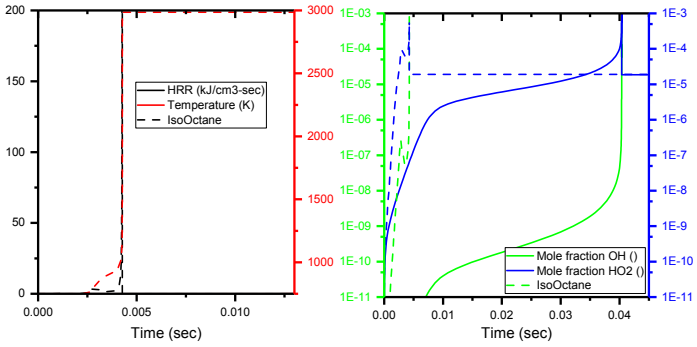

Figure B10: Reactivity evolution for mixture of 10% *n*-heptane and 90% *iso*-octane/ethanol. (a) heat release rate and temperature, (b) mole fraction of OH and HO_2. The values for ethanol-*n*-heptane are given in solid lines and *iso*-octane-*n*-heptane mixture are given in dashed lines.

Appendix 3:

The governing equations for a homogeneous constant volume auto-ignition are as follows:

$$\frac{d\boldsymbol{y}}{dt} = \frac{1}{\rho}\boldsymbol{W}\sum_{k=1}^{2K}\boldsymbol{S}_k R^k \tag{1}$$

$$\frac{dT}{dt} = \frac{1}{\rho C_v}\left(-\boldsymbol{h}_c\boldsymbol{W} + RT\boldsymbol{U}\right)\sum_{k=1}^{2K}R^k = \sum_{k=1}^{2K}v_k R^k \tag{2}$$

where y is the N-dimensional column vector of the species fraction, $\boldsymbol{S}_k$ and R^k represents the stoichiometric vector and reaction rate, respectively, of the k^{th} unidirectional reaction, ρ is the mixture density, $\boldsymbol{W}$ is the NxN diagonal matrix with the species molecular weights in the diagonal, C_v is the specific heat under constant volume, $\boldsymbol{h}_c$ is the N-dimensional vector of the species absolute enthalpies, T is the temperature, R is the universal gas constant, $\boldsymbol{U} = [1,1,\ldots,1]$ and v_k=$(-\boldsymbol{h}_c.\boldsymbol{W} + RT\boldsymbol{U})\boldsymbol{S}_k/(\rho C_v)$ [86, 87].

The above equations can be combined in CSP form as below:

$$\frac{d\boldsymbol{z}}{dt} = \boldsymbol{g}(\boldsymbol{z}) = \sum_{k=1}^{2K}\hat{\boldsymbol{S}}_k R^k = \sum_{n=1}^{N-E+1}\boldsymbol{a}_n f^n \tag{3}$$

where $\boldsymbol{z}$ is the (N+1)-dimensional state column vector, defined as $\mathbf{z} = [\boldsymbol{y}, T]^T$, $\hat{\boldsymbol{S}}_k$ is the (N+1)-dim. generalized stoichiometric column vector of the k-th reaction, $\boldsymbol{a}_n$ is the (N+1)–dim. CSP column basis vector of the n-th mode and f^n is the related amplitude and $f^n = \boldsymbol{b}^n.g(z)$ and $\boldsymbol{b}^i.\boldsymbol{a}_j = \delta^i_j$ [33, 34]. In the following, the CSP basis vectors a_n and b^n will be approximated by the right and left eigenvectors, respectively, of the Jacobian of $\mathrm{g(z)}$. The amplitudes f^{N-E+2} to f^{N+1} represent the conservation of the E elements and they are by definition zero. When the M fastest time scales of the system in Eq. 3 are exhausted, the system reduces to:

$$f^m \approx 0 \ (m = 1,\ldots, M) \qquad \frac{d\boldsymbol{z}}{dt} \approx \sum_{n=M+1}^{N-E+1} \boldsymbol{a}_n f^n \tag{4}$$

The algebraic M-dimensional system defines a low dimensional surface in tangent space, known as Slow invariant Manifold (SIM), on which the solution evolves according to the non-stiff (N+1)-dimensional system of ODEs [88, 89]. This system is free of the M fast time scales (τ_1 to τ_M) and its dynamics are characterized by the fastest of the slow (N-M-E+1) time scales, when the solution evolves sufficiently far from the boundaries of SIM [90, 91].

The time scales of the system in Eq. (3) are approximated by the relation $\tau_n = |\lambda_n|^{-1} (n = 2,\ldots,N-E+1)$, where $|\lambda_n|$ is the n-th nonzero eigenvalue of the Jacobian $\boldsymbol{J}$ of $\boldsymbol{g}(\boldsymbol{z})$.When the real part of λ_n is positive (negative), the related time scale τ_n is an explosive (dissipative) one, since it relates to components of the system that tend to lead it away from (towards to) equilibrium. The eigenvalue is defined as $\lambda_n = \boldsymbol{\beta}^n.\boldsymbol{J}.\boldsymbol{\alpha}_n$, where $\boldsymbol{\alpha}_n$ and $\boldsymbol{\beta}^n$ are the n-th right (column) and left (row), respectively, eigenvectors of $\boldsymbol{J}$. The n-th eigenvalue can be expressed as:

$$\lambda_n = \boldsymbol{\beta}^n.\sum_{k=1}^{2K} grad(\hat{\boldsymbol{S}}_k R^k).\boldsymbol{\alpha}_n = c_1^n + \ldots + c_{2K}^n \tag{5}$$

since $\boldsymbol{J} = grad(\hat{\boldsymbol{S}}_1 R^1) + \ldots + grad(\hat{\boldsymbol{S}}_{2K} R^{2K})$ [35, 44]. Considering the case where λ_n is real (the extension to the case where some of the eigenvalues are complex pairs is straightforward [92]), the expression in Eq. (5) suggests the introduction of the Time scale Participation index (TPI):

$$J_k^n = \frac{c_k^n}{|c_1^n| + \ldots + |c_{2K}^n|} \tag{6}$$

Where $n = 1,\ldots,N-E+1, k = 1,\ldots,2K$ and by definition $\sum_{k=1}^{2K} |J_k^n| = 1$. J_k^n measures the relative contribution of the k-th reaction to the n-th eigenvalue λ_n and, therefore, to the time scale τ_n. The J_k^n terms can be either positive or negative; positive (negative) J_k^n implies that the k -th reaction contributes to the explosive (dissipative) character of the n-th time scale τ_n. When the positive (negative) terms outweigh the negative (positive) ones the n-th time scale is an explosive (dissipative) one.

The TPI tool will be employed in order to investigate the origin of the fastest explosive time scale, say τ_e, that develops during the explosive stage of autoignition and relates to the fastest explosive CSP mode $\boldsymbol{a}_e f^e$ in Eq. (4) [35]. This stage is located at the start of the process and includes the period in which the explosive time scale is generated. The reactions that promote or oppose the development of τ_e will thus be identified with TPI. The significance of τ_e in autoignition processes, is based on the fact that the magnitude of the ignition delay t_{ign} is related to that of τ_e; i.e., $t_{ign} = O(\tau_e)$ [35, 48, 49, 64]. The variables (mass fractions

or the temperature) that (i) are being affected the most by τ_e, and (ii) are functionals in the reaction rates that contribute to the time scale τ_e and the amplitude f^e of the explosive mode will be identified with the CSP Pointer (Po), which is defined as:

$$\boldsymbol{D}^e = diagn\left[\boldsymbol{\alpha}_e\boldsymbol{\beta}^e\right] = \left[\alpha_e^1\beta_1^e,\ldots,\alpha_e^{N+1}\beta_{N+1}^e\right] \tag{7}$$

where by definition $\sum_{k=1}^{N}\alpha_e^k\beta_k^e = 1$. The magnitude of $D_k^e = \alpha_e^k\beta_k^e$ measures the relation of the k-th component of $\boldsymbol{z}$ to the time scale and amplitude of the explosive mode $\boldsymbol{a}_e f^e$ [64].